Exergy return on exergy investment analysis of natural-polymer (Guar-Arabic gum) enhanced oil recovery process

Hassan, Anas M.; Ayoub, M.; Eissa, M.; Musa, T.; Bruining, Hans; Farajzadeh, R.

DOI
10.1016/j.energy.2019.05.137

Publication date
2019

Document Version
Final published version

Published in
Energy

Citation (APA)
Hassan, A. M., Ayoub, M., Eissa, M., Musa, T., Bruining, H., & Farajzadeh, R. (2019). Exergy return on exergy investment analysis of natural-polymer (Guar-Arabic gum) enhanced oil recovery process. *Energy*, *181*, 162-172. https://doi.org/10.1016/j.energy.2019.05.137

Journal of Industrial and Engineering Chemistry 72 (2019) 133–143

Contents lists available at ScienceDirect

Journal of Industrial and Engineering Chemistry

journal homepage: www.elsevier.com/locate/jiec

A 2-D simulation study on CO_2 soluble surfactant for foam enhanced oil recovery

Yongchao Zeng[a], Rouhi Farajzadeh[b,c,*], Sibani L. Biswal[a], George J. Hirasaki[a]

[a] Rice University, 6100 Main St., MS-362, Department of Chemical and Biomolecular Engineering, Houston, TX, 77005 USA
[b] Shell Global Solutions International, 2288GS Rijswijk, The Netherlands
[c] Delft University of Technology, Delft, 2628CN, The Netherlands

ARTICLE INFO

Article history:
Received 3 October 2018
Received in revised form 25 November 2018
Accepted 6 December 2018
Available online 14 December 2018

Keywords:
Nonionic surfactant
Partition coefficient
CO_2
Foam
Gas breakthrough
Mobility control
Enhanced oil recovery (EOR)
Foam simulation

ABSTRACT

This paper probes the transport of CO_2 soluble surfactant for foaming in porous media. We numerically investigate the effect of surfactant partitioning between the aqueous phase and the gaseous phase on foam transport for subsurface applications when the surfactant is injected in the CO_2 phase. A 2-D reservoir simulation is developed to quantify the effect of surfactant partition coefficient on the displacement conformance and CO_2 sweep efficiency. A texture-implicit local-equilibrium foam model is embedded to describe how the partitioning of surfactant between water and CO_2 affects the CO_2 foam mobility control when surfactant is injected in the CO_2 phase. We conclude that when surfactant has approximately equal affinity to both the CO_2 and the water, the transport of surfactant is in line with the gas propagation and therefore the sweep efficiency is maximized. Too high affinity to water (small partition coefficient) results in surfactant retardation whereas too high affinity to CO_2 (large partition coefficient) leads to weak foam and insufficient mobility reduction. This work sheds light upon the design of water-alternating-gas-plus-surfactant-in-gas (WAG + S) process to improve the conventional foam process with surfactant-alternating-gas (SAG) injection mode during which significant amount of surfactant could possibly drain down by gravity before CO_2 slugs catch up to generate foam in situ the reservoir.

Introduction

CO_2 injection has superior displacement efficiency wherever gas contacts oil. It recovers oil by mechanisms of extraction, dissolution, solubilization, and possibly some other phase behavior changes [1–3]. As of 2017 in United States, it produces 280,000 barrels of oil per day accounting for approximately half of the oil produced by enhanced oil recovery (EOR) methods and 6% of the total domestic oil production [4–7]. With novel technologies being developed to capture CO_2 from industrial sites, CO_2 injection method is attracting more market interests. However due to the large density and viscosity contrast between CO_2 and the crude oil, the sweep efficiency of CO_2 flood is limited by gravity override and viscous fingering. The scenario could be worse if the reservoir is highly heterogeneous or fractured where the fluids of high mobility tend to finger through a preferential path and leave a large portion of the reservoir un-swept [2,8–16].

The sweep efficiency of CO_2 EOR can be improved by the injection mode of water-alternating-gas (WAG) [17–22]. Ideally the injected water can reduce the relative permeability of the CO_2 phase and therefore delay the gas breakthrough. However, the improvement can be limited because of phase segregation. A more potent way to reduce the mobility of CO_2 is to disperse the gas in aqueous phase with surfactants [8,23–30]. CO_2 Foam in porous media is a dispersion of CO_2 in aqueous phase such that the aqueous phase (wetting phase) is continuous and at least some part of the CO_2 (non-wetting phase) is made discontinuous by thin liquid films called lamella [31,8,32–35]. Depending on the reservoir temperature and pressure, CO_2 can be either gaseous-like or in the supercritical state. Above the critical temperature (31.10 °C) and pressure (1071 psi), gaseous CO_2 transitions into supercritical state. Conventional nomenclature refers to surfactant stabilized super critical CO_2 dispersion in water (C/W) as emulsion. Yet, for simplicity, we do not differentiate the gaseous-CO_2 foam and CO_2-in-water (C/W) emulsion [36] and only use the term CO_2 foam indicating that CO_2 is the internal phase. The rationale is that the fundamental principles of interfacial phenomena and transport properties as CO_2 foam transitions into CO_2 emulsion still hold the

* Corresponding author.
E-mail address: r.farajzadeh@tudelft.nl (R. Farajzadeh).

https://doi.org/10.1016/j.jiec.2018.12.013
1226-086X/

Nomenclature

C_{sg}	Surfactant concentration in the gaseous phase (g/L)
C_{sw}	Surfactant concentration in the aqueous phase (wt %)
epdry	Foam model parameter that regulates how abruptly foam dries out at limiting water saturation
epsurf	Foam model parameter, the exponent in $F_{surfactant}$ function
epoil	Foam model parameter, the exponent in F_{oil} function
F_{oil}	Oil dependent function in foam model
$F_{surfactant}$	Surfactant dependent function in foam model
F_{water}	Water saturation dependent function in foam model
floil	Foam model parameter that sets the maximum oil saturation below which the oil has no impact on foam
fmoil	Foam model parameter that sets the minimum oil saturation above which the oil kills the foam completely
FM	Correction factor function for gas phase mobility reduction by foam
fmmob	Foam model parameter that sets the maximum gas mobility reduction
fmsurf	Foam model parameter that sets the minimal surfactant concentration above which foam strength is no longer dependent on surfactant concentration
k_{rg}^{f}	Relative permeability to gas (foam)
k_{rg}^{nf}	Relative permeability to gas (no foam)
k_{rg}^{o}	End-point relative permeability to gas
k_{ro}	Relative permeability to oil
k_{rog}^{o}	End-point relative permeability to oil with respect to gas
k_{row}^{o}	End-point relative permeability to oil with respect to water
k_{rw}	Relative permeability to water
k_{rw}^{o}	End-point relative permeability to water
K_{sgw}	Surfactant partition coefficient between gaseous phase and aqueous phase
n_g	Corey exponent for gas
n_{og}	Corey exponent for oil with respect to gas
n_{ow}	Corey exponent for oil with respect to water
n_w	Corey exponent for water
PV	Pore volumes injected
S_g	Gas saturation
S_{gr}	Residual gas saturation
S_o	Oil saturation
S_{org}	Residual oil saturation to gas
S_{orw}	Residual oil saturation to water
S_w	Water saturation
S_{wc}	Connate water saturation
λ_{rg}^{f}	Mobility of the gas phase in presence of foam
λ_{rg}^{nf}	Mobility of the gas phase in absence of foam

same. Admittedly, as the density increases, CO_2 starts to solubilize crude oil. Nevertheless, the compositional change of the oleic phase during CO_2 flooding beyond minimal miscibility pressure (MMP) is beyond the scope of this paper. We mainly focus on the transport of CO_2 and surfactant in porous media.

Foam can decrease the mobility of CO_2 and increase the apparent viscosity of injection fluids by blocking the continuous gas path. Dispersed CO_2 bubbles trapped in the foam structure have a mobility that is orders of magnitude lower than continuous CO_2 flow. Therefore foam assisted CO_2 injection can effectively address the issue of poor mobility ratio and improve the volumetric sweep efficiency.

Commonly used ionic surfactants can only be injected in water because they are not soluble in the gas. Therefore the injection mode for these surfactants is called surfactant-alternating-gas (SAG). Well-known ionic surfactants have been introduced in detail from literature [26,29,37–41]. Novel CO_2 soluble surfactants include the nonionic exthoxylated alcohols and switchable exthoxylated amines [27,40,42–49]. The hydrophobic part can be either alkylphenol or branched/unbranched alkyl [45]. These surfactants can be injected with CO_2 phase. If surfactant is injected with CO_2, we call it water-alternating-gas-plus-surfactant-in-gas (WAG + S) mode. WAG + S process has the potential to outperform SAG in different ways. Firstly WAG + S can improve the well injectivity [50] when surface facilities switch from CO_2 injection to water injection. Secondly if surfactant is injected and transported in the CO_2 phase, it can foam with the water from secondary recovery, elongate the gas-water mixing zone and delay phase segregation [27,51–53].

Because the surfactant can dissolve in both the CO_2 and the water, it is critical to understand how the partitioning of the surfactant between the two phases can affect the foam transport in porous media. Partition coefficient K_{sgw} is a measure of the ratio in solubility of the surfactant in gaseous and aqueous phases. It is defined as the ratio of the surfactant concentration in gaseous phase C_{sg} to that in aqueous phase C_{sw} at thermodynamic equilibrium as in Eq. (1). In some literature, surfactant partition coefficient is defined as the ratio of mass fraction rather than the concentration. The two definitions of partition coefficient are different by a factor that equals to the density ratio of the two phases, yet represent the same in nature.

$$K_{sgw} = \frac{C_{sg}}{C_{sw}} \tag{1}$$

The value of surfactant partition coefficient K_{sgw} is dependent on several factors [27,38,54] and can be experimentally measured in the lab. Ren et al. [53] tested a series of different exthoxylated alcohols and discovered that the value of the partition coefficient of these CO_2 soluble surfactants varies in orders of magnitude with respect to the reservoir conditions (from 0.02 to greater than 1). In general, the partition coefficient increases proportionally with the reservoir pressure, whereas decreases more dramatically with the increase in reservoir temperature. Additionally, the K_{sgw} is very sensitive to surfactant formula and increases with decreasing ethylene oxide (EO) groups. The number of propylene oxide (PO) group also plays a critical role in determining surfactant partition coefficient. Compared to EO groups, PO group is more hydrophobic and tends to increase the K_{sgw}. Unlike nonionic surfactants, the partition coefficient of switchable surfactant is very sensitive to the reservoir pH. This is because the amine group can be protonated in the aqueous phase and the protonation degree increases with decreasing pH. This paper systematically simulates the transport of surfactant and foam in a 2-D homogeneous reservoir with different K_{sgw} values. In our previous paper [51], we established a 1-D 2-phase (water and CO_2) home-made foam simulator and demonstrated that when surfactant is approximately equally partitioning between gaseous phase and aqueous phase, foam is in favor for oil displacement in regard with apparent viscosity and foam propagation speed. In this paper, we extend the modeling to a 2-D 3-phase (water, CO_2, and oil) system with gravity at play. The simulation is done using Shell's in-house Modular Reservoir Simulator (MoReS) [55]. We will briefly summarize the implicit-texture (IT) local-equilibrium (LE) foam model in Section "Implicit-

texture local-equilibrium foam model", and review the three-phase relative permeability model in Section "Three-phase relative permeability model". We will introduce the 2-D homogeneous model reservoir created for simulation in Section "2-D Homogeneous model reservoir for simulation". In Section "CO_2 displacing water with different partition coefficients", we will discuss the effect of partition coefficient on foam by comparing the studied scenarios in which continuous CO_2 is injected with surfactants of varied partition coefficient into an aqueous reservoir to displace water. In Section "Case study: WAG, SAG and WAG + S", we will compare the oil recovery efficiency between WAG, SAG and WAG + S modes and will show that CO_2 soluble surfactants with proper partition coefficient can outperform conventional ionic surfactants in terms of mobility control and oil recovery efficiency by synchronizing the surfactant transport with gas phase propagation in a 2-D homogeneous model system.

Numerical models

Implicit-texture local-equilibrium foam model

Foam can lower the gas phase mobility by orders of magnitude. Yet the water mobility is proven to remain the same at a given water saturation [56]. Apparent viscosity μ_{app} is used as a measure of foam strength in porous media. It is defined as normalized pressure gradient ∇p with respect to rock permeability k and total superficial velocity $(u_g + u_w)$ as shown in Eq. (2).

$$\mu_{app} = -\frac{k \cdot \nabla p}{u_g + u_w} \tag{2}$$

The STARS version of the implicit-texture local-equilibrium model [57,58] implemented here modifies the relative mobility to the gas phase as shown in Eq. (3). The correction factor for the gas phase mobility reduction *FM* is inversely related to the product of a series of dependence functions as shown in Eq. (4). The parameter *fmmob* sets a reference to the maximum foam strength. The dependence functions $F_{surfactant}$, F_{water}, and F_{oil} are all in the range of [0,1]. The surfactant concentration dependence function $F_{surfactant}$ and the water saturation dependence function F_{water} are discussed in previous publications [59–62]. In Section "Case study: WAG, SAG and WAG + S" where the oil phase is present, function F_{oil} is introduced to account for the effect of oil on foam. Oil can destabilize foam in porous media by varied mechanisms [15,25,33,63,64]. In this simulation, the parameter *floil* represent the oil saturation below which oil does not affect foam strength and F_{oil} equals to 1, whereas the parameter *fmoil* represent the oil saturation above which foam is completely killed and F_{oil} equals to 0. The parameter *epoil* regulates how F_{oil} deceases as oil saturation S_o increases *floil to fmoil*. We list the values assigned to the parameters aforementioned in Table 1 and show the corresponding foam apparent viscosity as a function of foam quality (gas fractional flow $\frac{u_g}{u_g+u_w}$) and surfactant concentration C_{sw} in Fig. 1.

Table 1
STARS foam model parameters.

Parameter		Value
fmmob		500
$F_{surfactant}$	*fmsurf*	0.2 wt%
	epsurf	1
F_{wate}	*fmdry*	0.25
	epdry	500
F_{oil}	*floil*	0.1
	fmoil	0.4
	epoil	1.5

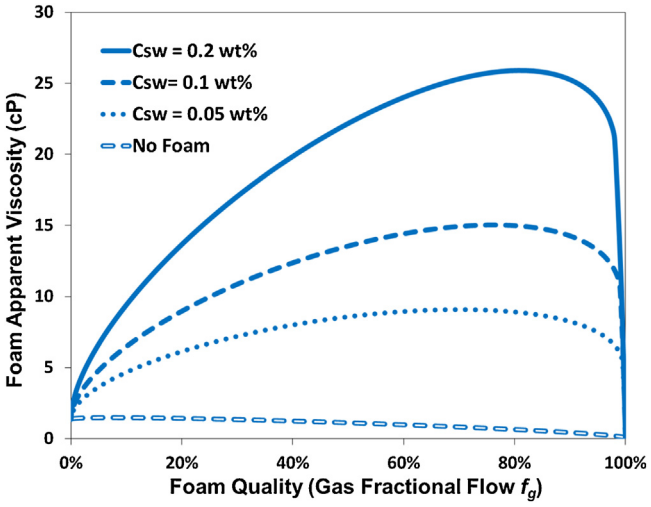

Fig. 1. Foam apparent viscosity μ_{app} calculated as a function of foam quality ($f_g = \frac{u_g}{u_g+u_w}$) and surfactant concentration C_{sw} using parameters aforementioned in Table 1.

$$\lambda_{rg}^{f} = \lambda_{rg}^{nf} \times FM \tag{3}$$

$$FM = \frac{1}{1 + fmmob \times F_{surfactant} \times F_{water} \times F_{oil}} \tag{4}$$

$$F_{surfactant} = \begin{cases} \left(\frac{C_{sw}}{fmsurf}\right)^{epsurf} & for C_{sw} < fmsurf \\ 1 & for C_{sw} \geq fmsurf \end{cases} \tag{5}$$

$$F_{water} = 0.5 + \frac{arctan[epdry(S_w - fmdry)]}{\pi} \tag{6}$$

$$F_{oil} = \begin{cases} 0 & for\, S_o > fmoil \\ \left(\frac{fmoil - S_o}{fmoil - floil}\right)^{epoil} & for\, floil < S_o < fmoil \\ 1 & for\, S_o < floil \end{cases} \tag{7}$$

Three-phase relative permeability model

Corey model [65] is used to calculate the relative permeability to water k_{rw} and gas k_{rg}^{nf} (no foam). It is well-known that formation wettability plays a critical role in determining the relative permeability curves [66–69]. Without introducing unnecessary complexities, we simply assume strict water-wet formation condition in this paper. Therefore, the parameter k_{rw} is only a function of water saturation S_w and k_{rg}^{nf} is only a function of gas saturation S_g. In the 3-phase simulation, linear iso-perm is applied to calculate the relative permeability to oil k_{ro} as shown in Fig. 2.

In the absence of gas, we use the water-oil two-phase Corey model to calculate k_{ro} based on the water/oil saturations (thick green line on the bottom); at connate water saturation (thick green line parallel to the side Gas–Oil), we use the Gas–Oil Corey model to calculate the k_{ro} at S_{wc}. In the three phase region, the linear iso-perm model assumes that the saturations (S_w, S_g, S_o) on the same tie line (straight lines connecting the two thick green lines) give the

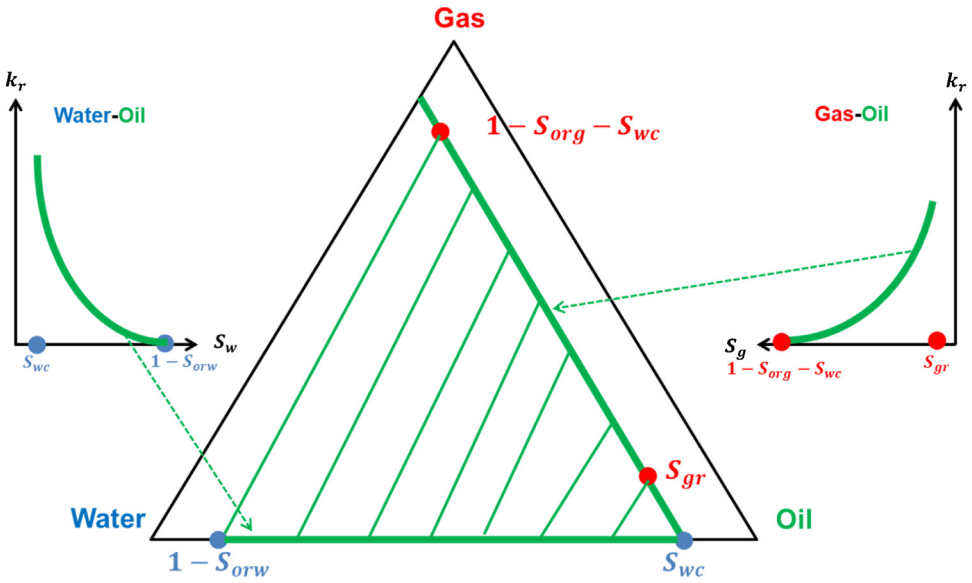

Fig. 2. Schematic of the linear iso-perm relative permeability to oil in 3-phase region.

same k_{ro} value. The three-phase relative permeability parameters are listed in Table 2.

2-D Homogeneous model reservoir for simulation

A 2-D homogeneous model reservoir with a permeability of 1 Darcy is created for the simulations in Section "CO_2 displacing water with different partition coefficients" and "Case study: WAG, SAG and WAG + S". The model reservoir is 2000 ft in length and 200 ft in thickness. Initially, the reservoir condition is set at 100 bar in pressure and 100 °C in temperature. In all cases studied, fluids are injected at 1 ft/day interstitial velocity. The Peclet numbers for the surfactant dispersion in both phases (CO_2 and water) are equal to 50 for field-level simulation [2].

In Section "CO_2 displacing water with different partition coefficients", the reservoir is initially 100% saturated with water. CO_2 is injected continuously with surfactant of different K_{sgw} values to displace the water as shown in Table 3. The injection surfactant concentration is 2.5 g/L CO_2 at reservoir conditions, 1.25 times of the *fmsurf* value. In this Section, we will focus on the effect of surfactant partitioning between CO_2 and aqueous phases on the surfactant transport and foam propagation, and investigate the optimal partition coefficient that maximizes the sweep efficiency of CO_2.

In Section "Case study: WAG, SAG and WAG + S", we add one more degree of complexity by introducing black oil into the model system. The hypothetical black oil has an API gravity of 45° and a viscosity of 0.4 cP under the reservoir condition (100 °C and 100 bar). The reservoir is initially at an oil saturation $S_{oi} = (1 - S_{wc})$ and the reservoir is water flooded for 1 PV before enhanced oil recovery techniques are applied. After the water flooding, the average oil saturation is reduced to 0.4. WAG, SAG, and WAG + S are applied to the water flooded reservoir respectively in Case A, B, and C. In this Section, we will focus on the comparison between these EOR applications.

Table 2
Three-phase relative permeability parameters to water, oil, and gas (no foam).

Water–oil relative permeability parameters		
Parameter	Symbol	Value
Connate water saturation	S_{wc}	0.10
Residual oil saturation to water	S_{orw}	0.40
End-point relative permeability to water	k^o_{rw}	0.22
End-point relative permeability to oil	k^o_{row}	1.0
Corey exponent for water	n_w	4.0
Corey exponent for oil with respect to water	n_{ow}	2.0
Oil–gas relative permeability parameters		
Parameter	Symbol	Value
Residual gas saturation	S_{gr}	0.05
Residual oil saturation to gas	S_{org}	0.01
End-point relative permeability to gas	k^o_{rg}	1.00
End-point relative permeability to oil	k^o_{rog}	k^o_{row}
Corey exponent for gas	n_g	1.7
Corey exponent for oil with respect to gas	n_{og}	4.0

Results and discussion

In this Section, we will first show the results of continuous CO_2 injection with CO_2 soluble surfactant to displace water and then compare the various EOR techniques, highlighting the benefit of injecting surfactant with CO_2 and the critical role of K_{sgw}.

CO_2 displacing water with different partition coefficients

In Case I, CO_2 with a CO_2 soluble surfactant of small partition coefficient ($K_{sgw} = 0.01$) is injected to displace water. The injected surfactant concentration is 2.5 g/L at reservoir condition. Fig. 3 displays the snapshots of the saturation and the surfactant concentration profile at different dimensionless times, the total pore volumes (PV) of CO_2 injected. It appears that the surfactant transport is severely retarded with respect to the gas propagation. After 1PV of injection, the surfactant only penetrates a fairly small portion of the reservoir. The segregation between the surfactant and the CO_2 is because of the extremely high surfactant affinity to water. Upon water contact, most of the surfactant quickly partitions into the aqueous phase. Therefore the surfactant accumulates in the near well-bore region and the surfactant concentration in the water C_{sw} is predominately higher than that in the gas phase C_{sg}. Once the surfactant is stripped off to the water, the CO_2 mobility control is lost. Consequently, the gas overrides the upper layer of the reservoir and streaks through early and the sweep of CO_2 is poor.

In Case II, the surfactant partition coefficient is set to 1, which means that the surfactant has equal affinity to both the CO_2 and the

Table 3
Characteristic values for surfactant partition coefficient K_{sgw} for the case studies in both Section "CO_2 displacing water with different partition coefficients" and Section "Case study: WAG, SAG and WAG + S".

Surfactant partition coefficient	Characteristic value	Remark
Small K_{sgw}	0.01	Strong affinity to water
Unity K_{sgw}	1.00	Equal affinity to water and CO_2
Large K_{sgw}	50.0	Strong affinity to CO_2

water. In contact with water, the surfactant concentration in the gas phase C_{sg} will be equal to that in the water C_{sw}. Fig. 4 shows the snapshots of the surfactant distribution along with the phase saturation profile. In this case, the surfactant transport is synchronized with the gas propagation. The surfactant creates foam with the water residing in the reservoir wherever the gas sweeps. The foamed gas can effectively mitigate the effect of gravity. Therefore, the sweep efficiency of CO_2 is greatly improved. After 1 PV of CO_2 injection, most of the reservoir has been swept.

In case III, the surfactant partition coefficient is increased to 50, which means that the surfactant prefers to stay with the CO_2 even

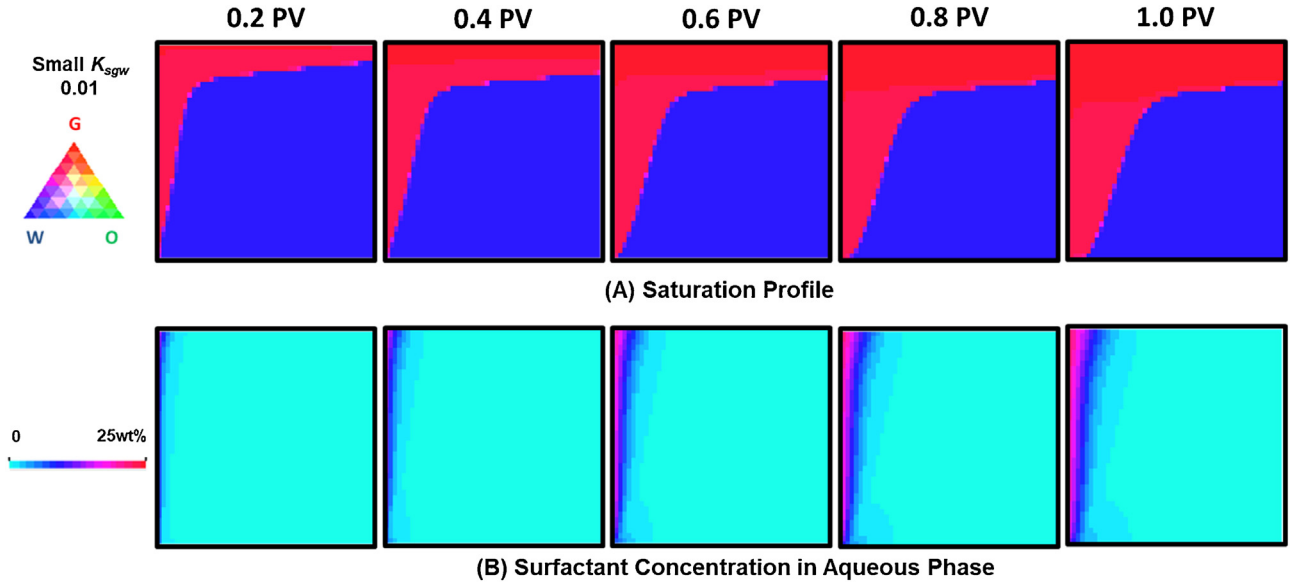

Fig. 3. Case I:Continuous CO_2 (with dissolved surfactant) injection to displace water with small partition coefficient K_{sgw} = 0.01 (A) Saturation profile indicating that the gas overrides the reservoir and prematurely breaks through; (B) Surfactant concentration profile indicating that the surfactant is highly concentrated near the well and the transport is retarded.

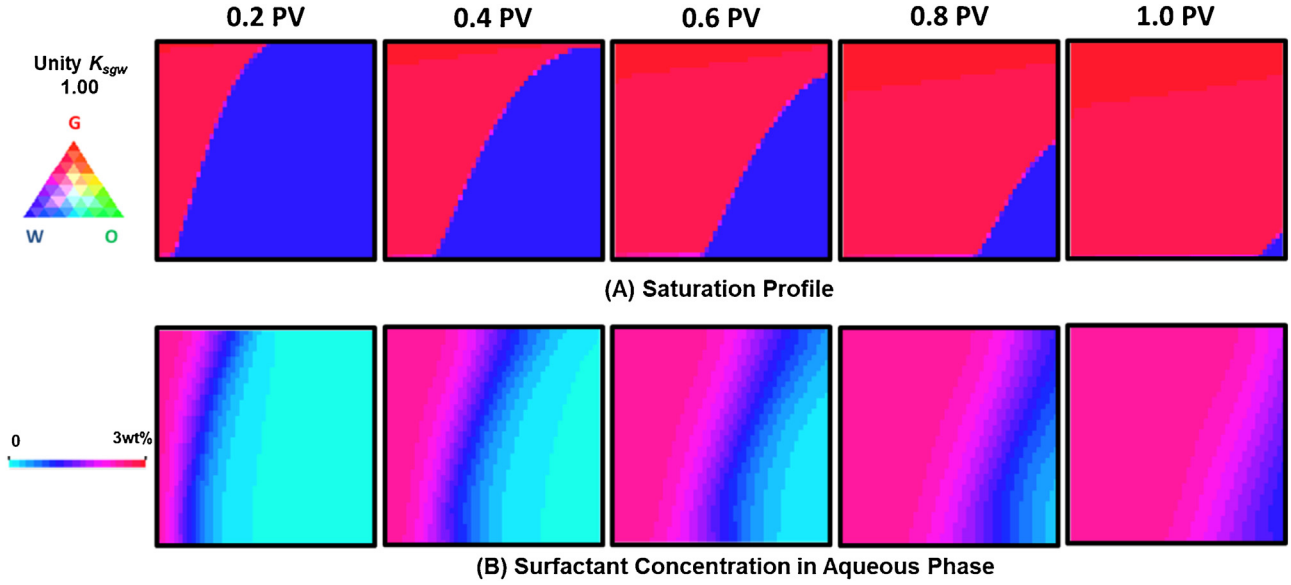

Fig. 4. Case II: Continuous CO_2 (with dissolved surfactant) injection to displace water with unity partition coefficient K_{sgw} = 1.00 (A) Saturation profile indicating that the sweep of CO_2 is greatly improved; (B) Surfactant concentration profile indicating that the surfactant transport is synchronized with the CO_2 propagation.

if it is equilibrated with water. At equilibrium, the surfactant concentration in the CO_2 C_{sg} will be a lot higher than that in the water C_{sw}. From $F_{surfactant}$ function, it is clear that foam strength is directly related to the C_{sw}. Therefore, the highly diluted surfactant concentration in the aqueous phase results in insufficient gas mobility reduction and the foam is not strong enough to fight against the gravity. Consequently, only the upper layer of the reservoir is swept by CO_2. Unlike Case I in which the CO_2 loses its mobility control completely, in Case III, the poor sweep efficiency results from the lack of surfactant in the aqueous phase as shown in Fig. 5.

From the case studies above, we conclude that the foam transport is highly dependent on the surfactant partition coefficient. Fig. 6 compares the water recovery efficiency with respect to different partition coefficient. Before the gas breakthrough, the efficiency of the water recovery is proportional to the volume of CO_2 injected. Therefore the three water recovery curves overlap in the beginning. In case of unity ($K_{sgw} = 1$) and large ($K_{sgw} = 50$) partition coefficients, most of the surfactant is carried by the CO_2. Therefore, after the CO_2 breaks through, the water recovery efficiency tends to level off and reach plateau. However, in the case of small partition coefficient ($K_{sgw} = 0.01$), the water recovery efficiency keeps increasing after the CO_2 breakthrough. This is due to the propagation of retarded surfactant bank. Because of the high affinity of the surfactant to the aqueous phase, water strips off the surfactant from the CO_2 soon after injection. Therefore, the surfactant front is left far behind the gas front. When the CO_2 reaches the production well at the breakthrough time, surfactant is still propagating in the reservoir. Therefore, more foam is being created and the water recovery efficiency keeps increasing. However, it takes much more volumes of CO_2 to reach the same level of water recovery efficiency compared to the case of unity partition coefficient.

In summary, unity partition coefficient is superior to either too large or too small partition coefficient in terms of mobility control and maximizing sweep efficiency. When the surfactant partition coefficient is too small, the surfactant will be highly concentrated near the well-bore, and the gas breaks through early. Too large partition coefficient result in weak foam, and the foam strength might not suffice to fight against gravity effect.

Case study: WAG, SAG and WAG + S

In this Section, we will compare three EOR techniques (Case A: WAG, Case B: SAG, and Case C: WAG + S) to demonstrate the advantage of using conventional foam and foam with CO_2 soluble surfactant for residual oil recovery. In all cases, the reservoir is water flooded to the remaining oil saturation of 0.4. In Case A, WAG, water slugs and gas slugs are alternatively injected into the reservoir. Each cycle consists of 0.2 PV of gas and 0.05 PV of water. In other words, the average gas fractional flow is 0.8. In Case B, SAG, 0.5 wt% of traditional surfactant (only soluble in water) is added to the aqueous phase to generate foam in situ. All the other operation conditions are kept exactly the same as Case A. In Case C, WAG + S, the same amount of CO_2 soluble surfactant is injected with CO_2 instead of water. The only difference between Case B and C is that in Case C, the surfactant is injected with the gas phase and partitions to the aqueous phase to foam with a partition coefficient of unity ($K_{sgw} = 1.0$). The foam model parameters in Case B and C are kept exactly the same, meaning that the surfactants have the same foaming capability.

Fig. 7 displays the 3-phase saturation profile snapshots for the WAG process. The gas only floods the upper part of the reservoir and breaks through during the first gas slug injection. The saturation profile does not change much after the first cycle is injected. Due to the density and viscosity contrast, the CO_2 pushes the oil down. An oil band is formed below the gas path way, however, is hardly produced due to the poor gas mobility control.

Foam can effectively mitigate the gravity effect. Fig. 8 shows the results of Case B in which 0.5 wt% surfactant (only soluble in water) is added to the aqueous phase. Gas mobility is significantly reduced by the generation of foam inside the porous medium. Gas (depicted in red) partially penetrates the lower part of the reservoir and an oil bank in green is formed in front of the foam. The oil is slowly produced from the production well on the right.

However, comparing the 3-phase saturation profile and the surfactant concentration profile in Fig. 8, it is noticed that significant amount of surfactant drains down before the gas slugs catches up and is wasted during the water injection period. The gas slug overrides the reservoir; however, the surfactant slug underrides the reservoir. A better alternative to inject the surfactant is

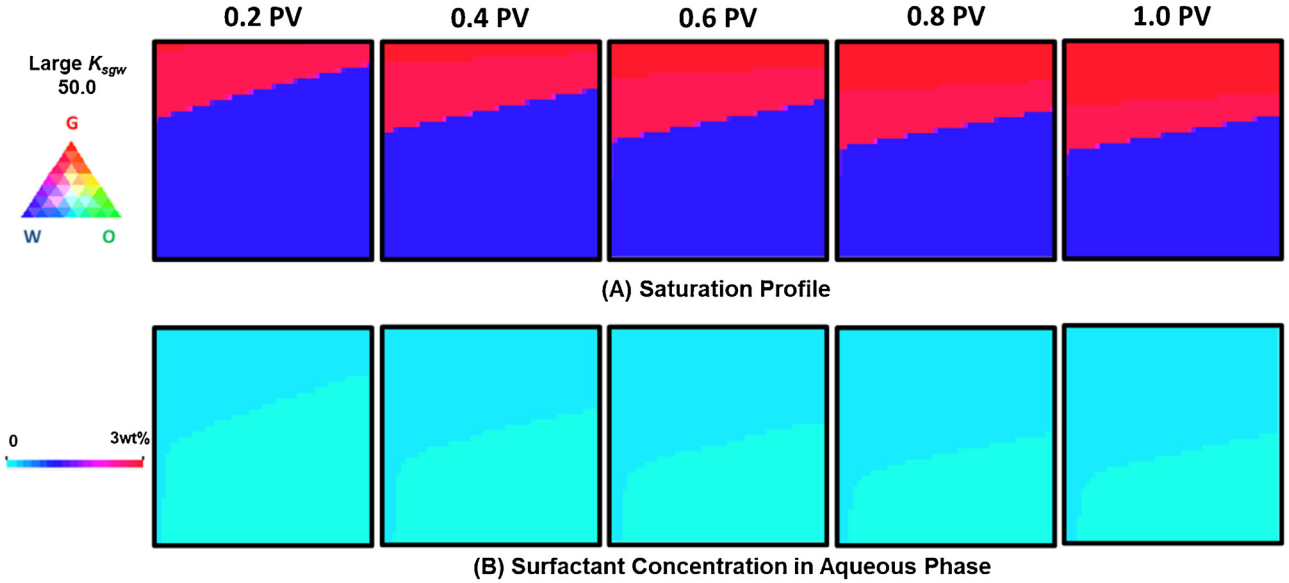

Fig. 5. Case III: Continuous CO_2 (with dissolved surfactant) injection to displace water with large partition coefficient of $K_{sgw} = 50.0$ (A) Saturation profile indicating that the foam strength is insufficient to keep CO_2 from overriding the reservoir; (B) Surfactant concentration profile indicating that the surfactant concentration in the aqueous phase is highly diluted.

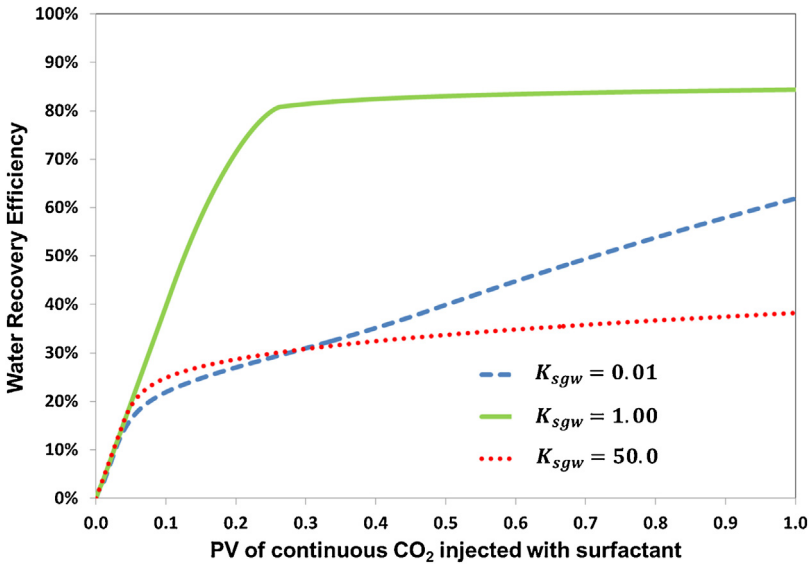

Fig. 6. Water recovery efficiency comparison between cases of varied surfactant partition coefficients. Unity partition coefficient is superior to either too small or too large partition coefficient in terms of water recovery efficiency.

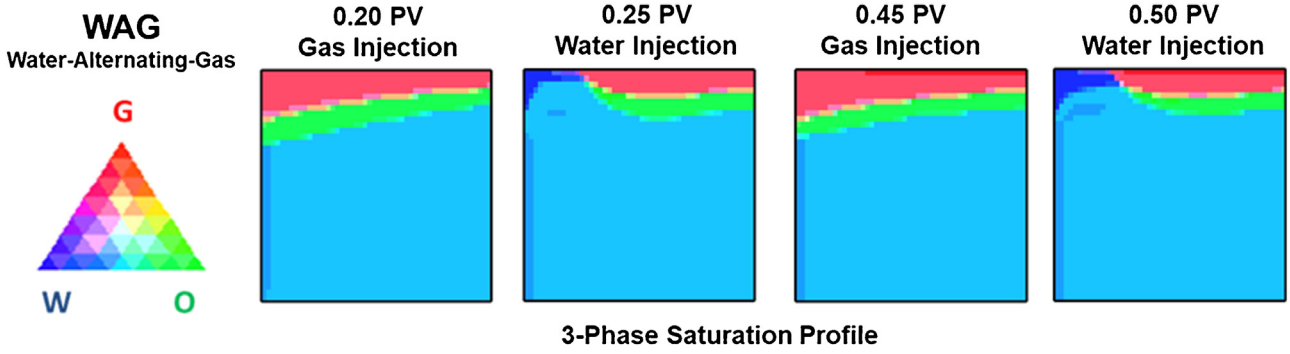

Fig. 7. Case A: Water-alternating-gas. The 3-phase saturation profile indicating that WAG mode has very limited improvement in oil recovery compared to waterflooding.

needed to synchronize the gas propagation and the surfactant transport such that the surfactant is available to make foam where the gas sweeps.

Fig. 9 displays the results when the same amount of surfactant is injected with the CO_2 phase instead of the water. The partition coefficient between the water and the CO_2 in this case is unity (K_{sgw} = 1.0). With the favorable partition coefficient, it is shown that the sweep is further improved from the SAG process. The gas phase carries the surfactant and dissolves the right amount to water to generate foam. It is notable that the gas penetrates into an even larger area in lower part of the reservoir. In addition, the oil bank accumulated is larger compared to the SAG process. All these improvement is because of the synchronization of the gas propagation and the surfactant transport.

However, it is important to point out that the recovery efficiency of WAG + S is highly dependent on the partition coefficient. As discussed in Section "CO_2 displacing water with different partition coefficients", too small partition coefficient results in surfactant transport retardation whereas too large partition coefficient results in insufficient foam robustness. As shown in Fig. 10(A), partition coefficient of either 0.01 or 50.0 leads to poorer oil recovery efficiency compared to SAG process. The sensitivity of surfactant partition coefficient on oil recovery is displayed in Fig. 10(B). The shape of the oil recovery efficiency curve, exhibiting a local maximum, is a result of the competing mechanisms between faster surfactant transport (large K_{sgw}) and higher foam strength (small K_{sgw}). The surfactant needs to be transported with the CO_2 whereas adequate amount of the surfactant needs to be dissolved in the water to make the foam strong. The optimized surfactant partition coefficient for WAG + S process is unity for the case considered here.

To further investigate the WAG + S process, a series of sensitivity analysis are conducted with respect to a number of critical reservoir properties such as crude oil viscosity, Peclet number/dispersivity, reservoir thickness, and well spacing (distance between the injection well and the production well). In all the sensitivity analysis, the reservoir is water-flooded for 1 PV and then the same WAG + S process as described above with a unity partition coefficient (K_{sgw} = 1.0) was applied. The overall oil recovery efficiency (crude oil percentage recovered based on the original oil in place (OOIP)) is plotted as a function of different variables as shown in Fig. 11.

Fig. 11(A) shows that the overall oil recovery efficiency is a strong function of the crude oil viscosity. As the crude oil viscosity increases, the efficiency of WAG + S process decreases linearly as a function of the logarithm of the crude oil viscosity using the same set of foam parameters. To generalize the observation, we define a new dimensionless variable called the oil/foamed gas viscosity ratio as shown in Eq. (8). The numerator is the crude oil viscosity μ_{oil} whereas the denominator is the gas viscosity μ_{gas} times the parameter *fmmob*. The denominator is a characteristic of the maximum foam strength (gas mobility reduction) that can be

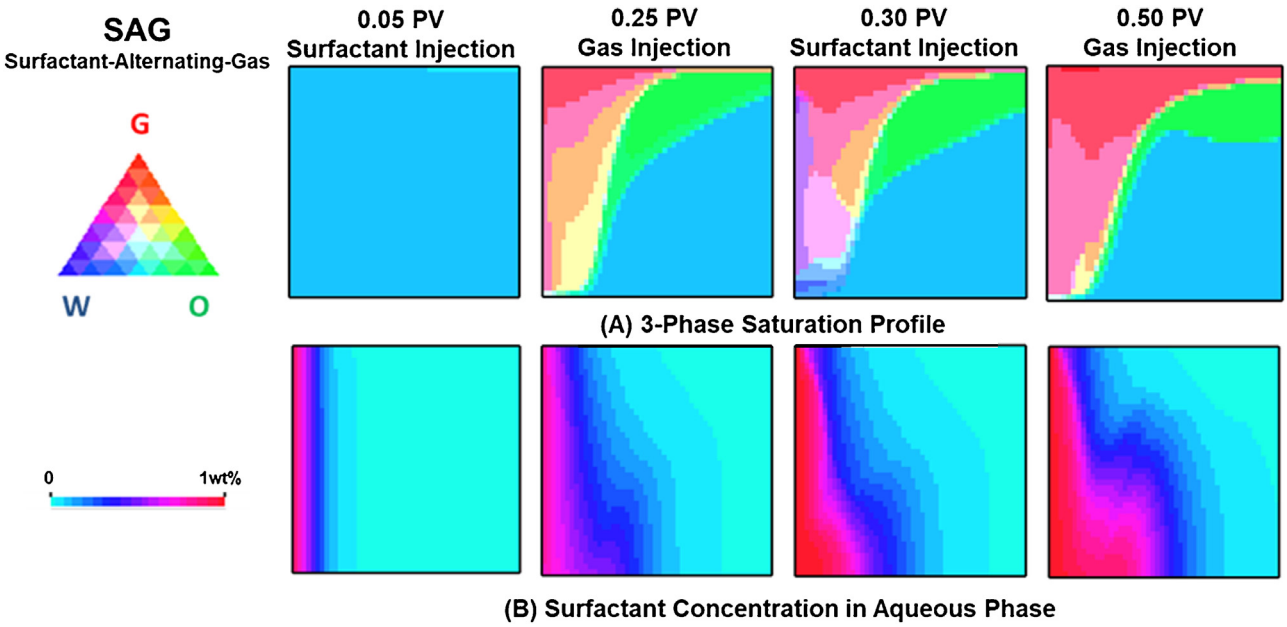

Fig. 8. Case B: Surfactant-alternating-gas. (A) 3-phase saturation profile indicating that the gas mobility is reduced by foam in presence of surfactant and the sweep efficiency is greatly improved from WAG injection. (B) Surfactant concentration profile indicating that significant surfactant drains by gravity before the CO_2 slug catches up. (For interpretation of the references to colour in the text, the reader is referred to the web version of this article.)

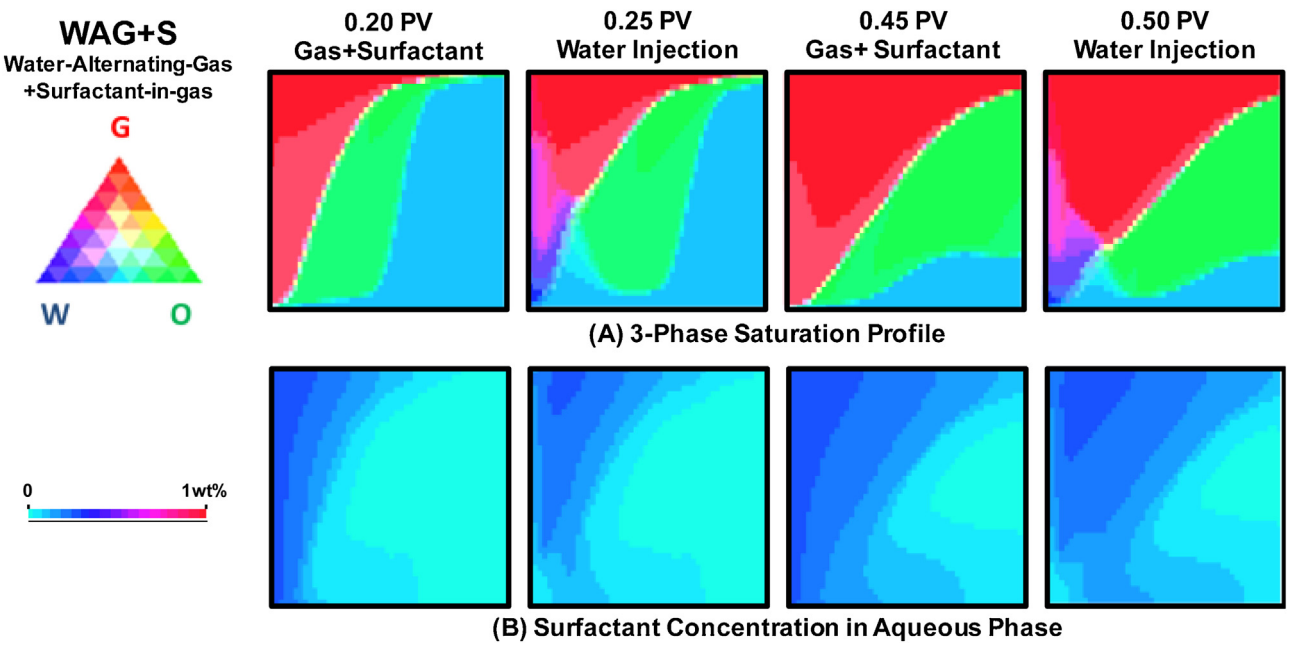

Fig. 9. Case C: Water-alternating-gas-plus-surfactant-in-gas. (A) 3-phase saturation profile indicating that a larger oil bank is formed and the oil recovery is further improved from SAG mode. (B) Surfactant concentration profile indicating that the surfactant transport is synchronized with the gas phase propagation.

expected. It is a simple measure of the relative viscosity of the crude oil and foam. It is concluded that stronger foam will be required as the crude oil viscosity increases in order to achieve a given oil recovery efficiency. Yet, it is worthwhile to mention that the crude oils of different viscosity are likely to have different foam-oil interactions. Therefore the parameters in the oil saturation dependent function F_{oil} are likely to vary. For simplicity, such effect is not included in this analysis.

$$\text{Oil/Foamed Gas Viscosity Ratio} = \frac{\mu_{oil}}{\mu_{gas} \times fmmob} \tag{8}$$

Fig. 11(B) shows the sensitivity analysis with respect to the dispersion. The overall oil recovery efficiency is plotted as a function of both the Peclet number and the dispersivity of the surfactant in the reservoir. It is well discussed in the literature [2] that the actual dispersivity of components increases with the characteristic length of the system. The reason behind is that the geological formations have heterogeneities of all length scales and thus mixing at all length scales. However, in this sensitivity analysis, it is found that the efficiency of WAG + S process is hardly affected by a wide change in the dispersivity values. In both lab scale and reservoir scale dispersion, the overall oil recovery

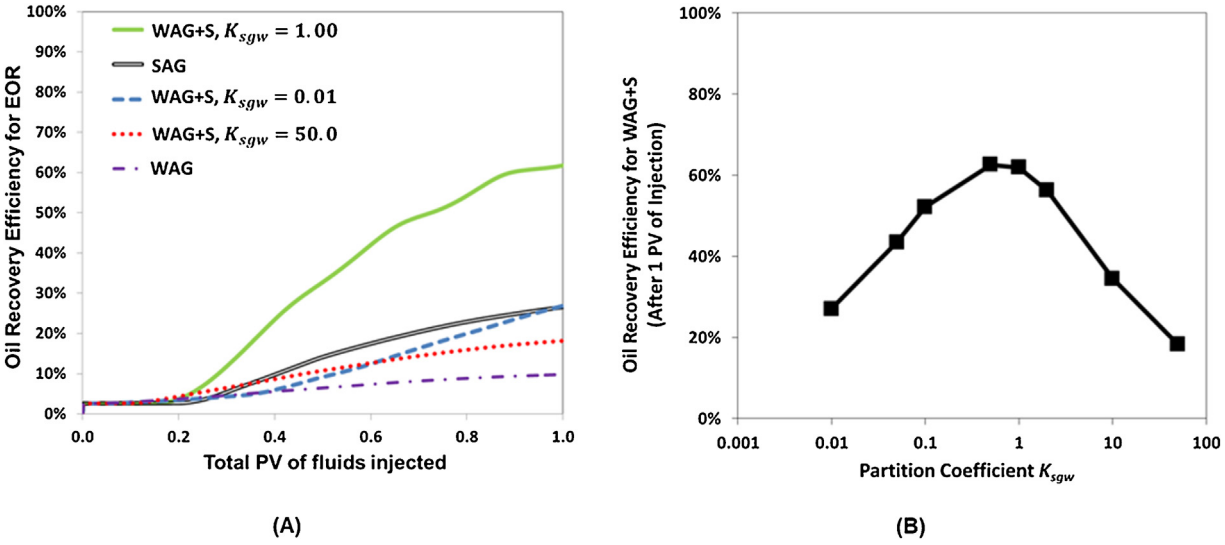

Fig. 10. (A) Oil recovery efficiency comparison between WAG, SAG, and WAG + S with varied partition coefficient. (b) Sensitivity of surfactant partition coefficient on WAG + S oil recovery efficiency.

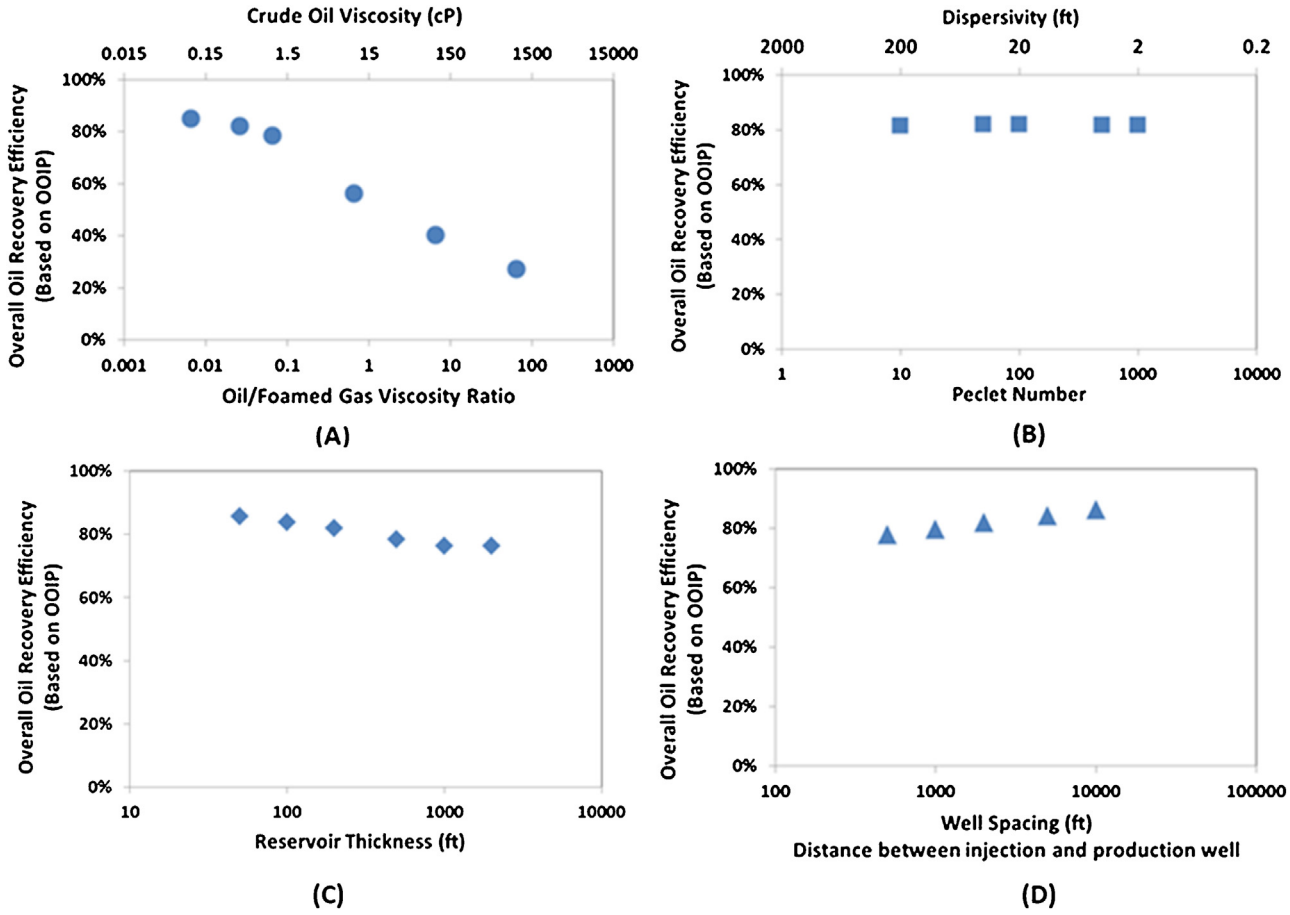

Fig. 11. Sensitivity analysis: (A) Overall oil recovery efficiency as function of crude oil viscosity and oil/foamed gas viscosity ratio. (B) Overall oil recovery efficiency as function of Peclet number and dispersity of the surfactant. (C) Overall oil recovery efficiency as function of reservoir thickness. (D) Overall oil recovery efficiency as function of well spacing (distance between injection and production wells).

efficiency is almost invariant as a function of the Peclet number and the dispersivity length scale. Yet, it is worthwhile to point out that the Peclet number can play a more pronounced role with small partition coefficient when surfactant is highly concentrated near the wellbore region. In that case, small Peclet number helps the transport/propagation of surfactant species and can potentially improve the sweep efficiency.

Fig. 11(C) and (D) show that the WAG + S foam process is also not very sensitive to the change in reservoir thickness and well spacing. As long as strong foam is generated in the presence of

crude oil, the process is effective across a wide range of reservoir dimensions. Admittedly, all our simulation is done at injection rate constraint. Sparse well spacing requires higher foam injectivity which might not be achievable at reservoir conditions.

Conclusions

We simulated the transport of CO_2 soluble surfactant in porous media and probed the effect surfactant partition coefficient on foam EOR. We firstly injected CO_2 with surfactant of different K_{sgw} values to a 100% water saturated reservoir. It is found out that the sweep of CO_2 is highly dependent on K_{sgw} values. Similar to our previous publication in 1-D system, when the surfactant has equal affinity to both the water and the gas, the sweep efficiency is optimized. A 2-D thick homogeneous reservoir with residual light oil was then set up for numerical simulation to probe the use of CO_2 soluble surfactant for foam EOR. In our case, WAG process has marginally better recovery efficiency compared to water flooding because of the low density and viscosity of the injected CO_2 phase. SAG process improves recovery efficiency by foaming the gas with surfactant solution and therefore providing mobility control. Yet, in the case of SAG injection, significant surfactant is wasted when the surfactant drains with the water before the following gas slug catches up to foam. A better alternative to SAG is WAG + S in which the surfactant is dissolved in the CO_2 phase and injected with gas instead of water. WAG + S can synchronize the transport of surfactant with the gas phase propagation when the partition coefficient is around 1. A series of sensitivity analysis were conducted to understand the efficiency and robustness of the WAG+S process. It is found that the oil recovery efficiency is a strong function of the crude oil viscosity or the oil/foamed gas viscosity ratio. However, the efficiency of the process is not severely impacted with changes in dispersion, reservoir thickness, and/or well spacing in our investigated range.

Conflict of interest

The authors declare no conflict of interest.

Acknowledgement

We acknowledge the financial support from Shell Global Solutions International (Rijswijk, Netherlands), Rice University Consortium in Processes in Porous Media (Houston, TX).

References

[1] V. Alvarado, E. Manrique, Energies 3 (9) (2010) 1529.
[2] L. Lake, R. Johns, W.R. Rossen, G. Pope, Soc. Pet. Eng. (2014).
[3] M. Orr. Franklin, Theory of Gas Injection Processes, Tie-Line Publications, Copenhagen, Denmark, 2017.
[4] V.A. Kuuskraa, M.L. Godec, P. Dipietro, Energy Procedia 37 (2013) 6854.
[5] D. Hussain, D.A. Dzombak, P. Jaramillo, G.V. Lowry, Int. J. Greenh. Gas Control 16 (2013) 129.
[6] P. Jaramillo, W.M. Griffin, S.T. McCoy, Environ. Sci. Technol. 43 (21) (2009) 8027.
[7] Y. Zeng, A Multiscale Study of Foam: The Phase Behavior, Transport, and Rheology of Foam in Porous Media. Ph.D. Thesis, Rice University, 6100 Main St, Houston, TX, 2017 77005.
[8] A.R. Kovscek, C.J. Radke, Foams Fundamentals and Applications in the Petroleum Industry, vol. 242, American Chemical Society, 1994.
[9] S.I. Kam, W. Rossen, SPE J. 8 (04) (2003) 417.
[10] C.A. Conn, K. Ma, G.J. Hirasaki, S.L. Biswal, Lab Chip 14 (20) (2014) 3968.
[11] R.F. Li, W. Yan, S. Liu, G. Hirasaki, C.A. Miller, SPE J. 15 (04) (2010) 928.
[12] M.A. Fernø, L.P. Hauge, A. Uno Rognmo, J. Gauteplass, A. Graue, Geophys. Res. Lett. 42 (18) (2015) 7414.
[13] M.A. Fernø, Ø. Eide, M. Steinsbø, S.A.W. Langlo, A. Christophersen, A. Skibenes, T. Ydstebø, A. Graue, J. Pet. Sci. Eng. 135 (2015) 442.
[14] R. Singh, K. Mohanty, Fuel 197 (2017) 58.
[15] S. Xiao, Y. Zeng, E.D. Vavra, P. He, M.C. Puerto, G.J. Hirasaki, S.L. Biswal, Langmuir 34 (3) (2017) 739.
[16] P. Dong, M. Puerto, G. Jian, K. Ma, K. Mateen, G. Ren, G. Bourdarot, D. Morel, M. Bourrel, S.L. Biswal, et al., SPE J. (2018).
[17] M.M. Kulkarni, D.N. Rao, J. Pet. Sci. Eng. 48 (1–2) (2005) 1.
[18] M.F. Sedaralit, N.B. Darman, R.D. Tewari, R.Z. Kamarul Bahrim, P. Abdul Hamid, S.R. Mohd Shafian, A.A. Abdul Manap, Enhancing the Efficiency of Immiscible Water Alternating Gas (WAG) Injection in a Matured, High Temperature and High CO2 Solution Gas Reservoir - A Laboratory Study, SPE Enhanced Oil Recovery Conference, 2–4 July, Kuala Lumpur, Malaysia, 2013 (165303-MS).
[19] M. Sohrabi, D.H. Tehrani, A. Danesh, G.D. Henderson, SPE J. 9 (03) (2004) 290.
[20] J.D. Rogers, R.B. Grigg, SPE Reservior Eval. Eng. 4 (05) (2001) 375.
[21] L. Han, Y. Gu, Energy Fuels 28 (11) (2014) 6811.
[22] H. Lei, S. Yang, L. Zu, Z. Wang, Y. Li, Energy Fuels 30 (11) (2016) 8922.
[23] T. Blaker, M.G. Aarra, A. Skauge, L. Rasmussen, H.K. Celius, H.A. Martinsen, F. Vassenden, SPE Reservior Eval. Eng. 5 (04) (2002) 317.
[24] A.H. Falls, J.B. Lawson, G.J. Hirasaki, J. Pet. Technol. 40 (01) (1988) 95.
[25] K. Mannhardt, I. Svorstøl, J. Pet. Sci. Eng. 23 (3–4) (1999) 189.
[26] L. Cui, K. Ma, M. Puerto, A.A. Abdala, I. Tanakov, L.J. Lu, Y. Chen, A. Elhag, K.P. Johnston, S.L. Biswal, et al., SPE J. (2016).
[27] G. Ren, Q.P. Nguyen, Pet. Sci. (2017).
[28] S. Kahrobaei, S. Vincent-Bonnieu, R. Farajzadeh, Sci. Rep. 7 (1) (2017).
[29] G.J. Hirasaki, C.A. Miller, M. Puerto, et al., Recent Advances in Surfactant EOR, SPE Annual Technical Conference and Exhibition, 21–24 September, Denver, Colorado, USA, 2008 (SPE-115386-MS).
[30] G.J. Hirasaki, C.A. Miller, R. Szafranski, J.B. Lawson, N. Akiya, Surfactant/Foam Process for Aquifer Remediation, International Symposium on Oilfield Chemistry, Houston, Texas, 1997 18–21 February, (SPE-37257-MS).
[31] S. Alzobaidi, C. Da, V. Tran, M. Prodanović, K.P. Johnston, J. Colloid Interface Sci. 488 (2017) 79.
[32] A. Al Sumaiti, A.R. Shaik, E.S. Mathew, W. Al Ameri, Energy Fuels 31 (5) (2017) 4637.
[33] R. Farajzadeh, A. Andrianov, R. Krastev, G.J. Hirasaki, W.R. Rossen, Adv. Colloid Interface Sci. 183–184 (0) (2012) 1.
[34] Y. Zeng, R. Farajzadeh, A.A. Eftekhari, S. Vincent-Bonnieu, A. Muthuswamy, W. R. Rossen, G.J. Hirasaki, S.L. Biswal, Langmuir (2016).
[35] Y. Zeng, R.Z.K. Bahrim, S.V. Bonnieu, J. Groenenboom, S.R.M. Shafian, A.A.A. Manap, R.D. Tewari, S.L. Biswal, Offshore Technology Conference Asia, Kuala Lumpur, Malaysia, 20-23 March, The Dependence of Methane Foam Transport on Rock Permeabilities and Foam Simulation on Fluid Diversion in Heterogeneous Model Reservoir, 20–232018 (OTC-28229-MS).
[36] S. Kahrobaei, K. Li, S. Vincent-Bonnieu, R. Farajzadeh, AIChE J. 64 (2) (2018) 758.
[37] K. Mannhardt, J.J. Novosad, K.N.N. Jha, J. Can. Pet. Technol. 33 (02) (1994).
[38] Y. Chen, A.S. Elhag, L. Cui, A.J. Worthen, P.P. Reddy, J.A. Noguera, A.M. Ou, K. Ma, M. Puerto, G.J. Hirasaki, et al., Ind. Eng. Chem. Res. 54 (16) (2015) 4252.
[39] M. Chorro, N. Kamenka, B. Faucompre, S. Partyka, M. Lindheimer, R. Zana, Colloids Surf. Physicochem. Eng. Aspects 110 (3) (1996) 249.
[40] G. Jian, M.C. Puerto, A. Wehowsky, P. Dong, K.P. Johnston, G.J. Hirasaki, S. Biswal, Langmuir 32 (40) (2016) 10244.
[41] G. Jian, M. Puerto, A. Wehowsky, C. Miller, G.J. Hirasaki, S.L. Biswal, J. Colloid Interface Sci. 513 (2018) 684, doi:http://dx.doi.org/10.1016/j.jcis.2017.11.041.
[42] Y. Chen, A.S. Elhag, B.M. Poon, L. Cui, K. Ma, S.Y. Liao, P.P. Reddy, A.J. Worthen, G. J. Hirasaki, Q.P. Nguyen, et al., SPE J. 19 (02) (2014) 249.
[43] A.S. Elhag, Y. Chen, H. Chen, P.P. Reddy, L. Cui, A.J. Worthen, K. Ma, G.J. Hirasaki, Q.P. Nguyen, S.L. Biswal, et al., Switchable Amine Surfactants for Stable C/Brine Foams in High Temperature, High Salinity Reservoirs SPE Improved Oil Recovery Symposium, Tulsa, Oklahoma, USA 12-16 April, 2014 (SPE -169041-MS).
[44] L. Cui, K. Ma, A.A. Abdala, L.J. Lu, I. Tanakov, S.L. Biswal, G.J. Hirasaki, Adsorption of a Switchable Cationic Surfactant on Natural Carbonate Minerals; SPE Improved Oil Recovery Symposium, Tulsa, Oklahoma, USA, 12-16 April, 2014 (SPE -169040-MS).
[45] D. Xing, B. Wei, W.J. McLendon, R.M. Enick, S. McNulty, K. Trickett, A. Mohamed, S. Cummings, J. Eastoe, S. Rogers, et al., SPE J. 17 (04) (2012) 1172.
[46] Y. Zhang, L. Zhang, Y. Wang, M. Wang, Y. Wang, S. Ren, Chem. Eng. Res. Des. 94 (2015) 624.
[47] Y. Wang, Y. Zhang, Y. Liu, L. Zhang, S. Ren, J. Lu, X. Wang, N. Fan, J. Pet. Sci. Eng. 154 (2017) 234.
[48] Y. Zhang, Y. Wang, F. Xue, Y. Wang, B. Ren, L. Zhang, S. Ren, J. Pet. Sci. Eng. 133 (2015) 838, doi:http://dx.doi.org/10.1016/j.petrol.2015.04.003.
[49] S.S. Adkins, X. Chen, I. Chan, E. Torino, Q.P. Nguyen, A.W. Sanders, K.P. Johnston, Langmuir 26 (8) (2010).
[50] D. Shan, W.R. Rossen, Optimal Injection Strategies for Foam IOR; SPE/DOE Improved Oil Recovery Symposium, Tulsa, Oklahoma, 13-17 April, 2002 (SPE-75180-MS).
[51] Y. Zeng, K. Ma, R. Farajzadeh, M. Puerto, S.L. Biswal, G.J. Hirasaki, Transp. Porous Media (2016).
[52] E. Ashoori, T. van der Heijden, W.R. Rossen, Fractional Flow Theory of Foam Displacements With Oil, SPE International Symposium on Oilfield Chemistry The Woodlands. Texas 20-22 April, 2009 (SPE -121579-MS).
[53] G. Ren, A.W. Sanders, Q.P. Nguyen, J. Supercrit. Fluids 91 (2014) 77.
[54] C.T. Lee, P.A. Psathas, K.P. Johnston, J. deGrazia, T.W. Randolph, Langmuir 15 (20) (1999) 6781.
[55] J.M.M. Regtien, G.J.A. Por, M.T. van Stiphout, F.F. van der Vlugt, Interactive Reservoir Simulation, SPE Reservoir Simulation Symposium San Antonio, Texas 12-15 February, 1995 (SPE -29146-MS).
[56] A.A. Eftekhari, R. Farajzadeh, Sci. Rep. 7 (2017) 43870.
[57] K. Ma, G. Ren, K. Mateen, D. Morel, P. Cordelier, SPE J. 20 (03) (2015) 453.
[58] M. Lotfollahi, R. Farajzadeh, M. Delshad, A. Varavei, W.R. Rossen, J. Nat. Gas Sci. Eng. 31 (2016) 184.
[59] K. Ma, J.L. Lopez-Salinas, M.C. Puerto, C.A. Miller, S.L. Biswal, G. Hirasaki, Energy Fuels 27 (5) (2013) 2363.

[60] Y. Zeng, A. Muthuswamy, K. Ma, L. Wang, R. Farajzadeh, M. Puerto, S. Vincent-Bonnieu, A.A. Eftekhari, Y. Wang, C. Da, et al., Ind. Eng. Chem. Res. 55 (28) (2016) 7819.
[61] O.G. Apaydin, A.R. Kovscek, Transient Foam Flow in Homogeneous Porous Media: Surfactant Concentration and Capillary End Effects, SPE/DOE Improved Oil Recovery Symposium Tulsa, Oklahoma 3-5 April, 2000 (SPE -59286-MS).
[62] B. Géraud, S.A. Jones, I. Cantat, B. Dollet, Y. Méheust, Water Resour. Res. 52 (2) (2016) 773.
[63] M. Amirmoshiri, Y. Zeng, Z. Chen, P.M. Singer, M.C. Puerto, H. Grier, R.Z.K. Bahrim, S. Vincent-Bonnieu, R. Farajzadeh, S.L. Biswal, et al., Energy Fuels 32 (11) (2018) 11177.
[64] E.D. Vavra, Y. Zeng, S. Xiao, G.J. Hirasaki, S.L. Biswal, J. Visualized Exp. (131) (2018).
[65] A.T. Corey, Prod. Mon. (19) (1954) 38.
[66] W. Abdallah, J.S. Buckley, A. Carnegie, J. Edwards, B. Herold, E. Fordham, A. Graue, T. Habashy, N. Seleznev, C. Signer, et al., Technology 38 (1125–1144) (1986) 268.
[67] G. Hirasaki, Wettability Fundamentals and Surface Forces, vol. 6(1991) SPE Formation Evaluation Issue 02, June (SPE-17367-PA).
[68] J. Song, Y. Zeng, L. Wang, X. Duan, M. Puerto, W.G. Chapman, S.L. Biswal, G.J. Hirasaki, J. Colloid Interface Sci. 506 (2017) 169.
[69] B.M. Lescure, E.L. Claridge, CO2 Foam Flooding Performance vs. Rock Wettability, SPE Annual Technical Conference and Exhibition, New Orleans, Louisiana, 5-8 October, 1986 (SPE-15445-MS).